Materials Science | Special Issue 150 Years of BASF

DOI: 10.1002/anie.201410139

Biologically Inspired Dynamic Material Systems

*André R. Studart**

Keywords:
bio-inspired materials · dynamic material systems · materials science · organic–inorganic hybrid composites · responsive materials

Angewandte International Edition Chemie

Numerous examples of material systems that dynamically interact with and adapt to the surrounding environment are found in nature, from hair-based mechanoreceptors in animals to self-shaping seed dispersal units in plants to remodeling bone in vertebrates. Inspired by such fascinating biological structures, a wide range of synthetic material systems have been created to replicate the design concepts of dynamic natural architectures. Examples of biological structures and their man-made counterparts are herein revisited to illustrate how dynamic and adaptive responses emerge from the intimate microscale combination of building blocks with intrinsic nanoscale properties. By using top-down photolithographic methods and bottom-up assembly approaches, biologically inspired dynamic material systems have been created 1) to sense liquid flow with hair-inspired micro-electromechanical systems, 2) to autonomously change shape by utilizing plantlike heterogeneous architectures, 3) to homeostatically influence the surrounding environment through self-regulating adaptive surfaces, and 4) to spatially concentrate chemical species by using synthetic microcompartments. The ever-increasing complexity and remarkable functionalities of such synthetic systems offer an encouraging perspective to the rich set of dynamic and adaptive properties that can potentially be implemented in future man-made material systems.

From the Contents

1. Introduction

Dynamic material systems (DynMatS) refer to biological and engineering assemblies that enable sensing, interaction with, or adaptation to the surrounding environment. The working principles and underlying mechanisms leading to such dynamic responses usually differ markedly in biological and conventional man-made systems.

In nature, dynamic and adaptive behavior often emerge from the cooperative interactions of building blocks of different chemical properties and geometries assembled in hierarchical architectures over multiple length scales. For example, chemically driven molecular motors work cooperatively to control several fundamental biological processes within living cells including cargo transport, cell division, and cell motility.[1,2] The dynamics enabled by such molecular motors allow cells to actively interact with and control their surrounding environment to perform all the vital functions of an organism.[3] Ultimately, cells are combined into tissues and organs at the next hierarchical levels to perform specific macroscopic functions, from mechanical support and locomotion to homeostasis and mental activity. Despite the relatively narrow range of chemical elements utilized in biological systems, the power of the hierarchical structuring approach observed in nature is evident from the diversity of dynamic living organisms present in the natural world.[4]

In contrast to the hierarchical structuring and cooperative interaction between building blocks in the living world, conventional engineered systems often rely on materials with specific chemical properties that undergo phase transitions at the atomic/molecular scale to enable macroscopic dynamic behavior in the form of piezoelectric, pyroelectric, electrochromic, shape-memory effects, to name just a few of the numerous examples.[5–7] Despite the myriad of adaptive and interactive properties achievable and their widespread use in many man-devised technologies,[8,9] most engineered DynMatS lack the intimate organization of the building blocks, with their different chemical properties, at multiple length scales, as found in their biological counterparts. For example, piezoelectric macroscopic components generate an electrical signal in response to a mechanical stimulus through the stress-induced relative displacement of electrical charges, a phenomenon arising intrinsically from the atomic length scale.[10] Likewise, macroscopic parts made from NiTi alloys and polymers close to the glass transition rely on atomic and molecular phase transitions to obtain the shape memory effect required to recover their original shape after being mechanically deformed to arbitrary geometries.[6,7] The limited availability of specific chemical compounds that undergo the aforementioned atomic/molecular transitions is a major constraint in the development of engineered DynMatS.

As the chemistry and organization of biological and synthetic structures are so distinct, many of the design principles underlying the multiscale architecture of biological systems may be exploited synthetically to achieve engineered systems with new functionalities. Moreover, the implementation of natural hierarchical structures in synthetic systems

[*] Prof. A. R. Studart
Complex Materials, Department of Materials
ETH Zürich, 8093 Zürich (Switzerland)

may diminish their dependence on specific, often environmentally hazardous, chemical reactions to achieve the desired responses. Although they differ significantly from the elegant cell-controlled biological processes found in natural systems, several fabrication technologies have been devised to successfully mimic biological design concepts in engineered systems with unprecedented properties.[11–24] Recent reviews have discussed biological materials and bio-inspired counterparts that exhibit outstanding mechanical behavior, but which do not significantly change their structures and properties over time and can thus be referred to as "static" architectures.[11,12]

In this Review, examples of biological and bio-inspired material systems are revisited that dynamically and reversibly change their structure and properties in response to an external stimulus. The selected examples are not comprehensive. Instead, they were chosen to illustrate the increasing level of complexity that has been pursued to synthetically realize some of the dynamic functionalities of hierarchical biological material systems. Although major efforts have been dedicated to the creation of nanomachines inspired by biological molecular motors,[2,25] focus is paid to developments that stretch beyond the nanoscale to reach micro- and eventually macroscopic dimensions. The dynamic response of the selected examples can range widely in frequency, from slow diffusion-controlled motions to higher-frequency oscillatory systems.

Earlier and ongoing research that attempts to replicate artificially the sensorial properties of biological hair cells are considered first. Since these biological material systems are often present on or close to open surfaces, their translation into engineered systems has greatly benefited from advanced photolithographic techniques originally developed to structure surfaces in the semiconductor industry. The availability of such mature fabrication methods resulted in the development of artificial hair and cilia being one of the earliest in biomimetic research. The next example concerns synthetic systems that are able to dynamically change their shape through the diffusion-controlled anisotropic contraction/expansion properties programmed within the extracellular matrix of plant tissues. As opposed to most sensorial hair systems, such self-shaping DynMatS can exhibit dynamic features in the absence of cellular intervention. The last example discusses current attempts to create synthetic microcapsules that might enable the future realization of very primitive sensing and actuating functions of living cells in an artificial engineered system. Despite the complexity required and the many challenges involved, these compartmentalized structures might allow the possibility to design DynMatS that adapt and remodel their internal architecture similar to the regeneration and remodeling processes observed in biological systems. The remodeling ability of bone is discussed in the closing section to illustrate the formidable dynamic material systems that nature can build to generate cell-based adaptive response in a load-bearing structural material.

André R. Studart obtained his PhD at the Federal University of São Carlos, Brazil. From 2002 and 2007 he was a postdoctoral and senior scientist at ETH Zurich, where he studied the mechanical properties of dental ceramics and the processing of porous materials through colloidal routes. In 2007 he joined Harvard University to work on porous inorganic materials obtained using microfluidic techniques. Since 2009 he has been professor at ETH Zurich and heads the Complex Materials group in the Department of Materials. His research concerns bio-inspired composites and complex materials with potential applications as medical implants, energy conversion systems, and smart structures.

2. Sensorial Hair Cells

Hair cells are used for mechanosensory purposes in many living organisms across the animal kingdom, ranging from insects and spiders to fish and mammals.[26–28] The basic structure of hair cells is highly conserved across these very different animals (Figure 1 a). This biological sensing system usually comprises a hair bundle that is connected with the apical surface of the cell at one end and has most of its length exposed to the environment.[29] The hair bundle is formed by a long filament called a kinocilium and progressively smaller adjacent filaments known as stereovilli (Figure 1 a). Sensing takes place when the stereovilli are deflected relative to the kinocilium by airflow or touch, which results in electrical depolarization or hyperpolarization across the lipid membrane of the underlying cell. Polarization is detected by nerve endings connected at the bottom of the hair cell. The intensity and direction of the environmental stimulus (airflow or touch) is measured by the extent to which the hair bundle is deflected and thus the level of polarization detected across the cell membrane. In such a system, hair bundles interact with the cellular membrane at the microscale to generate the nanoscale electrical displacement necessary for sensing. Using this sensing mechanism, hair cells can perform a wide variety of sensorial functions, including the detection of infrared, sound pressure, gravity, and angular acceleration.[29]

The hair cells used in the sensorial system of fish, known as the fish lateral line, are used here as an illustrative example of the design rules underlying such mechanoreceptors. Fish exhibit two types of sensing receptors along the lateral line: the superficial and the canal neuromasts (Figure 1 b), both based on the hair cell structure described above (Figure 1 a).[26,29] Superficial neuromasts are exposed on the surface of the fish and are directly exposed to the surrounding environment, whereas the canal neuromasts are located inside a subdermal canal along the lateral line at mid-positions between orifices on the fish's skin. The distribution of neuromasts over the fish skin can vary significantly in different species. An example of the distribution of such mechanosensory elements throughout the body of a teleost fish is shown in Figure 1 b.

Fish use these mechanoreceptors for the detection of approaching predators, identification of nearby prey, localization of objects, schooling, and rheotaxis.[30,31] For example, surface-feeding fish can detect waves created by insects on free water surfaces at distances up to three times their own

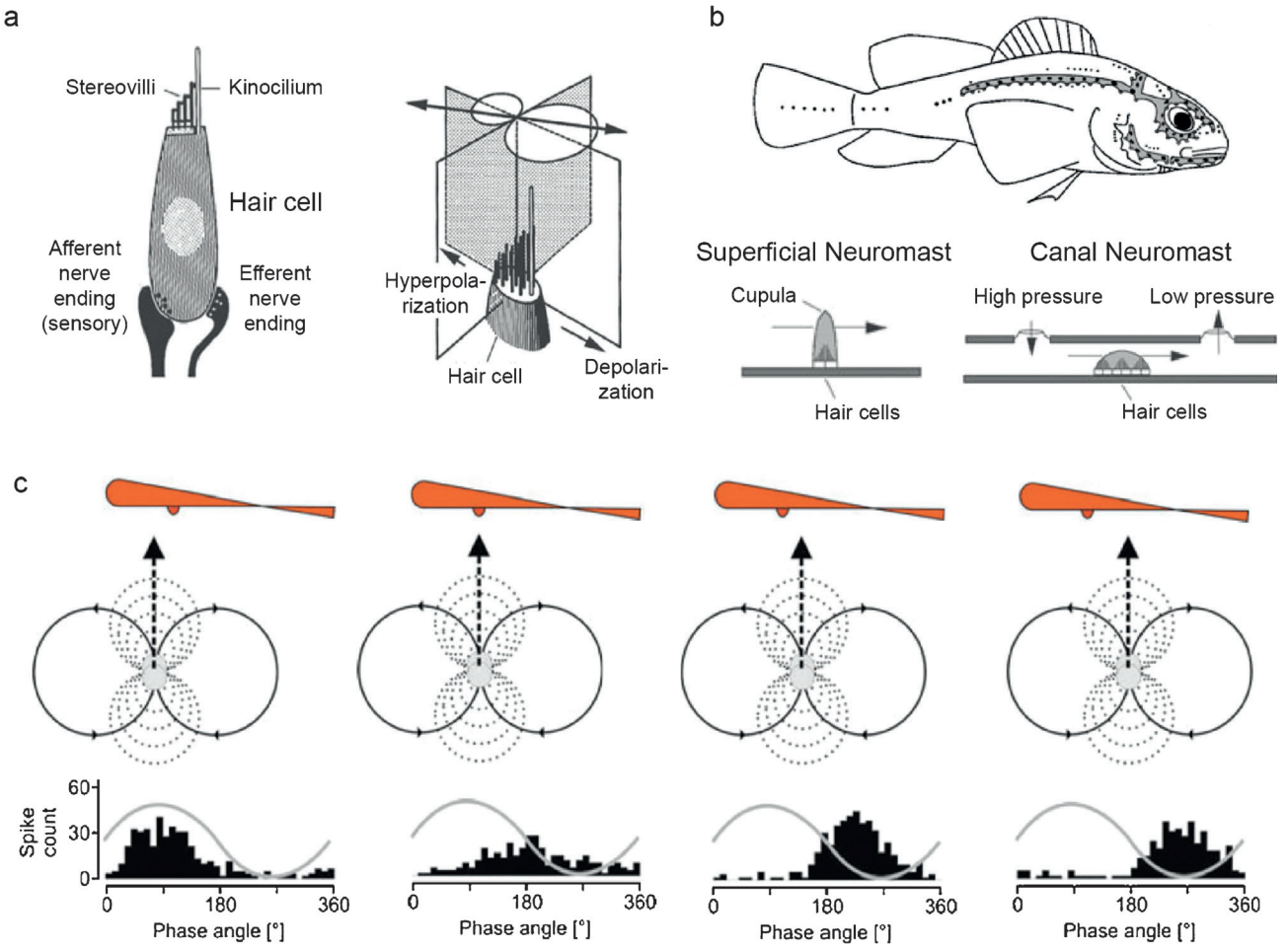

Figure 1. The mechanoreceptor system of fish.[29] a) Basic structure of the hair cell, indicating the cell membrane polarization arising from the deflection of the stereovilli. Adapted with permission from Bleckmann et al.[29] b) Example of the distribution of mechanoreceptors on the skin of a teleost fish. The two types of mechanoreceptors, the superficial and canal neuromasts, are indicated by dots within the light and gray areas, respectively. Adapted with permission from Bleckmann et al.[29] and Coombs.[102] c) Electrical signal detected by a hair cell in water as an oscillating sphere (flow dipole) passes along the fish lateral line. Adapted with permission from Bleckmann et al.[29]

body length.[29] Several studies have been performed to understand the effect of different types of continuous (DC) or oscillatory (AC) flow patterns on the electrical response of neuromasts along the lateral line. Figure 1c shows the response of lateral line neuromasts of a fish to the pressure waves created by a moving oscillating sphere. The results indicate that the phase of the oscillatory signal detected by a neuromast shifts continuously from 0 to 180° as the wave source moves laterally along the fish. This illustrates a possible approach used by fish to detect the direction and speed of objects moving under water. Researchers speculate that the ability of a fish to probe its hydrodynamic environment extends far beyond the detection of the motion of a single object. By using arrays of thousands of superficial and canal neuromasts distributed over the head, body, and tail fins,[32] fish are likely able to collect enough spatial and temporal data to enable 3D visualization of their environment based solely on the hydrodynamic stimuli captured by their sensorial hair system.

The translation of some of the design concepts of the fish mechanosensory system into synthetic systems is expected to generate advanced sensing approaches with several envisaged applications. This ranges from novel sensing arrays for the controlled navigation of unmanned vehicles to local probing of wall shear stresses for a deeper understanding of turbulence and other complex hydrodynamic phenomena. Taking advantage of well-established lithographic processes for the structuring of surfaces, different microelectromechanical systems (MEMS) have been proposed to mimic the basic structure of hair cells (Figure 1a).[33,34] Similar to the biological structure, the basic detection principle of most synthetic systems also relies on the generation of an electrical signal at the nanoscale in response to the deflection of a single element or bundle of the hair at the microscale. In the two exemplary synthetic systems discussed here, the electrical signal is generated by deforming a capacitive element (Figure 2) or a piezoelectric film (Figure 3) underneath the artificial hair.

The capacitive artificial hair senses flow in the surrounding environment by detecting changes in the capacitance between electrode pairs under the hair (Figure 2a).[35,36] Changes in capacitance are measured relative to an adjacent reference electrode to ensure signal stability at different

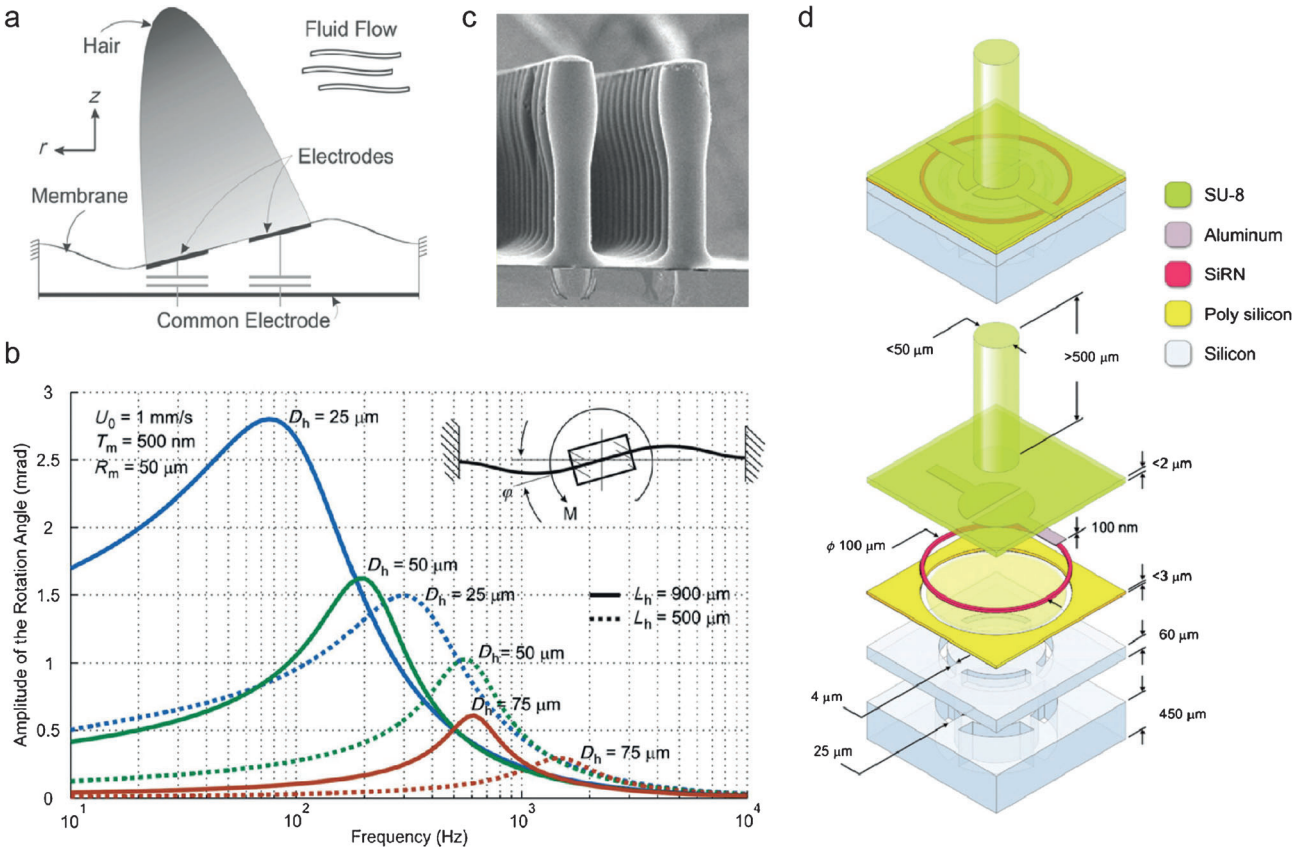

Figure 2. Synthetic hairlike capacitive sensor inspired by the fish lateral line.[35,36] a) Basic working principle of the sensor, indicating the change in the electrode separation as the artificial hair is deflected by the flow. b) Calculated magnitude of the rotation angle (ϕ) of a synthetic hair as a function of frequency for different hair geometries. D_h: hair diameter; L_h: hair length; U_0: flow velocity; M: flow-induced torque; T_m: membrane thickness; R_m: membrane diameter. c) Array of synthetic polymer hairs made from an epoxy-based photoresist (SU-8) through photolithography. d) Example of the combination of different materials and geometries required for the fabrication of a synthetic hairlike sensor. SiRN: silicon-rich silicon nitride. (a)–(c) were adapted with permission from Izadi and Krijnen.[35] (d) was adapted with permission from Izadi et al.[36]

temperatures. Mechanical modeling of the entire hair system reveals that the detectable frequency range and frequency of maximum sensitivity can be tuned by changing the aspect ratio of the hair element (Figure 2b). In addition to this geometrical factor, higher sensitivity also requires the use of a soft and easily deformable membrane beneath the hair element. To fulfill these specific geometrical and mechanical demands and also to provide the electrical properties required for the capacitor components, the bio-inspired sensing device has, inevitably, to be fabricated from a combination of various materials. In the specific example depicted schematically in Figure 2d, the materials are thin polymeric membranes (epoxy-based photoresist SU-8) to enhance the device sensitivity to electrical insulators (air and silicon-rich silicon nitride) and conductors (aluminum and silicon) to build the capacitor layers. In addition to single sensing elements, MEMS comprising arrays of multiple artificial hairs have been fabricated by using this lithographic approach (Figure 2c).

Silicon-based lithography has also been exploited to fabricate piezoresistive artificial hair sensors.[32,37] In this case, a polymeric hair is typically mounted on a silicon-based piezoresistive cantilever, which changes its electrical resistance upon deflection of the hair (Figure 3a,b). Recently, these sensors have been utilized to systematically investigate the noise-filtering ability of canal neuromasts in an artificial system. Synthetic analogues of the canal neuromast were built by covering a row of piezoresistive artificial hairs with a poly(dimethyl siloxane) (PDMS) layer with a semicircular long opening and equidistant periodic surface pores (Figure 3c). Such artificial canal neuromasts were compared with a superficial neuromast analogue by exposing the sensors to a regular oscillatory (dipole) hydrodynamic stimulus superimposed with a turbulent flow of various increasing intensities (Figure 3d). In the absence of turbulent flow, the two types of sensors can effectively detect the oscillatory flow at the well-defined frequency of 20 Hz. When exposed to the strongest superimposed turbulent flow, the single superficial hair senses all the random oscillations and loses its ability to detect the regular oscillatory object. In contrast, the artificial canal neuromast is unaffected by the turbulent flow and remains sensitive to the periodic stimulus regardless of the intensity of the background noise. This finding provides insights into the selectivity and sensing characteristics of canal and superficial neuromasts. The above underwater hair sensors illustrate how different materials and geometries can be combined in dynamic material systems to either enable the detection of minute flow stimuli or selectively sense important hydro-

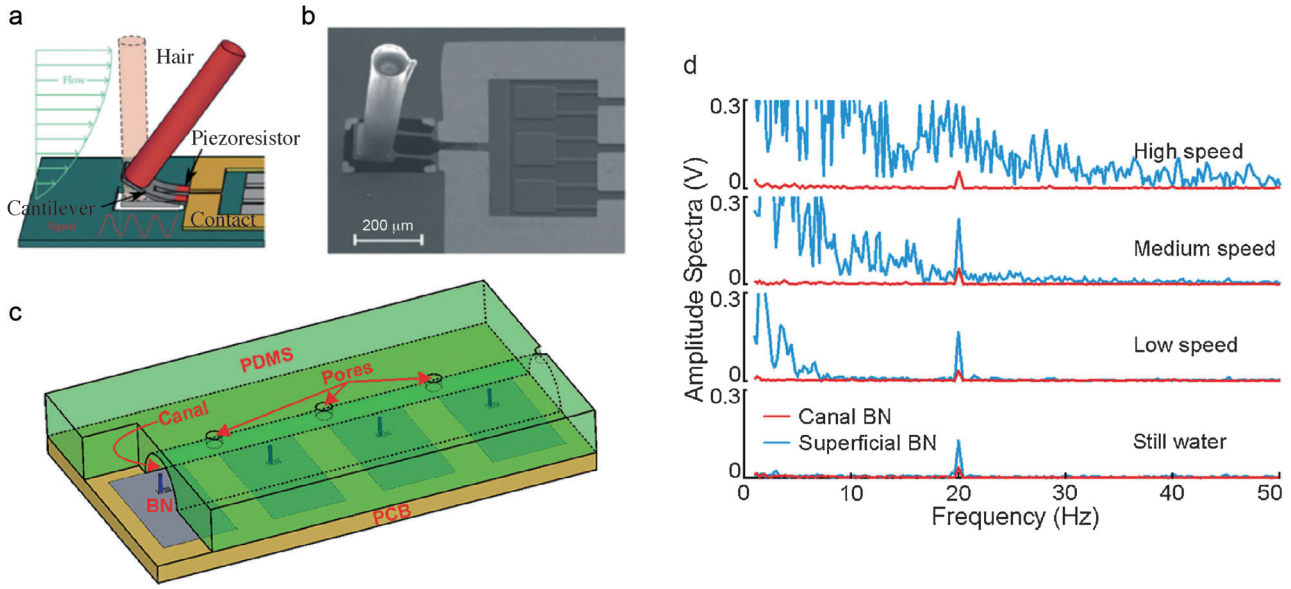

Figure 3. Synthetic hairlike piezoresistive sensor inspired by the fish lateral line.[32,37] a) Schematic representation showing the working principle of a piezoresistive cantilever that is deflected together with the hair element in the presence of flow. Adapted with permission from Nguyen et al.[37] b) Scanning electron micrograph of an actual piezoresistive sensor that mimics a superficial neuromast. c) Schematic representation of a synthetic analogue of a lateral line with canal neuromasts. d) Electrical signals detected at different frequencies by artificial analogues of a superficial and a canal neuromast when exposed to a periodic flow pattern at 20 Hz superimposed with turbulent flow with increasing intensities. (b)–(d) were adapted with permission from Yang et al.[32]

dynamic signals through effective filtering of background noise.

3. Autonomous Shape-Changing Systems

Although the information detected by biological hair sensors is further processed by a nervous system before deliberate action of the organism, several examples exist of dynamic material systems that can autonomously actuate in direct response to a sensing event.[28] This direct coupling between sensing and actuation is observed in many plant systems that are programmmed to change shape and release their seeds upon variations in the humidity of the environment (Figure 4).[18,38–41] For example, pinecones and certain seedpods release seeds by bending and twisting valves, respectively, when they disconnect from water-replenishing branches and eventually dry (Figure 4 a–e). In another case, wetting rather than drying the plant dispersal unit can induce a shape change. This is the case of some ice plants living in arid or semi-arid habitats, which increase their chances of germination by opening their valves to release seeds only in the rare event of a rainy day (Figure 4 f–h).[38] In contrast to other shape-changing plants, such as the well-known Venus trap,[42] the externally triggered shape change of pinecones, seedpods and ice-plant seed capsules occur in the absence of cellular control. This implies that the shape change occurs autonomously and is totally programmed within the microstructure of the system through the combination of building blocks of different intrinsic properties and length scales.

The mechanism of the shape change is determined by the microstructure programmed by the plant cells. In pinecones and chiral seedpods, shape change is achieved by constructing bilayer-like valves comprising a swellable hemicellulose matrix that is reinforced with cellulose fibrils that have a distinct orientation in each individual layer.[41,43] Such a site-specific orientation of the fibrils causes the individual layers to shrink differently during the drying of the bilayer valve. As the fibrils mechanically reinforce the hemicellulose matrix, layers shrink more strongly in directions perpendicular to the orientation of the reinforcement. In the simplified representation of a pinecone valve shown in Figure 4 c, it is evident that the fibril architecture is organized such that the bottom layer is only reinforced in the out-of-plane direction and thus shrinks more strongly during drying than does the in-plane reinforced top layer. As a result, a bending motion is observed upon drying. A similar reinforced bilayer concept is found in the architecture of chiral seedpods (Figure 4 e). The cellulose fibrils in each of the seedpod layers are also aligned orthogonally to one another, but in this case the reinforcement in each layer occurs at an angle of 45° with respect to the long axis of the seedpod. This fibril architecture makes a twisting configuration the most energetically favored geometry upon drying-induced shrinkage of the individual layers.[41] In both cases, the macroscopic shape change arises from the removal of water molecules from solvated hemicellulose at the nanoscale combined with the anisotropic swelling effect generated by the oriented reinforcement architecture at the microscale.

In contrast to the deliberate fibril architectures found in pinecones and chiral seedpods, the ice-plant seed capsule depicted in Figure 4 f–h relies on the water-triggered anisotropic swelling of hexagonal-shaped cells as the main mechanism leading to autonomous shape change.[21] This

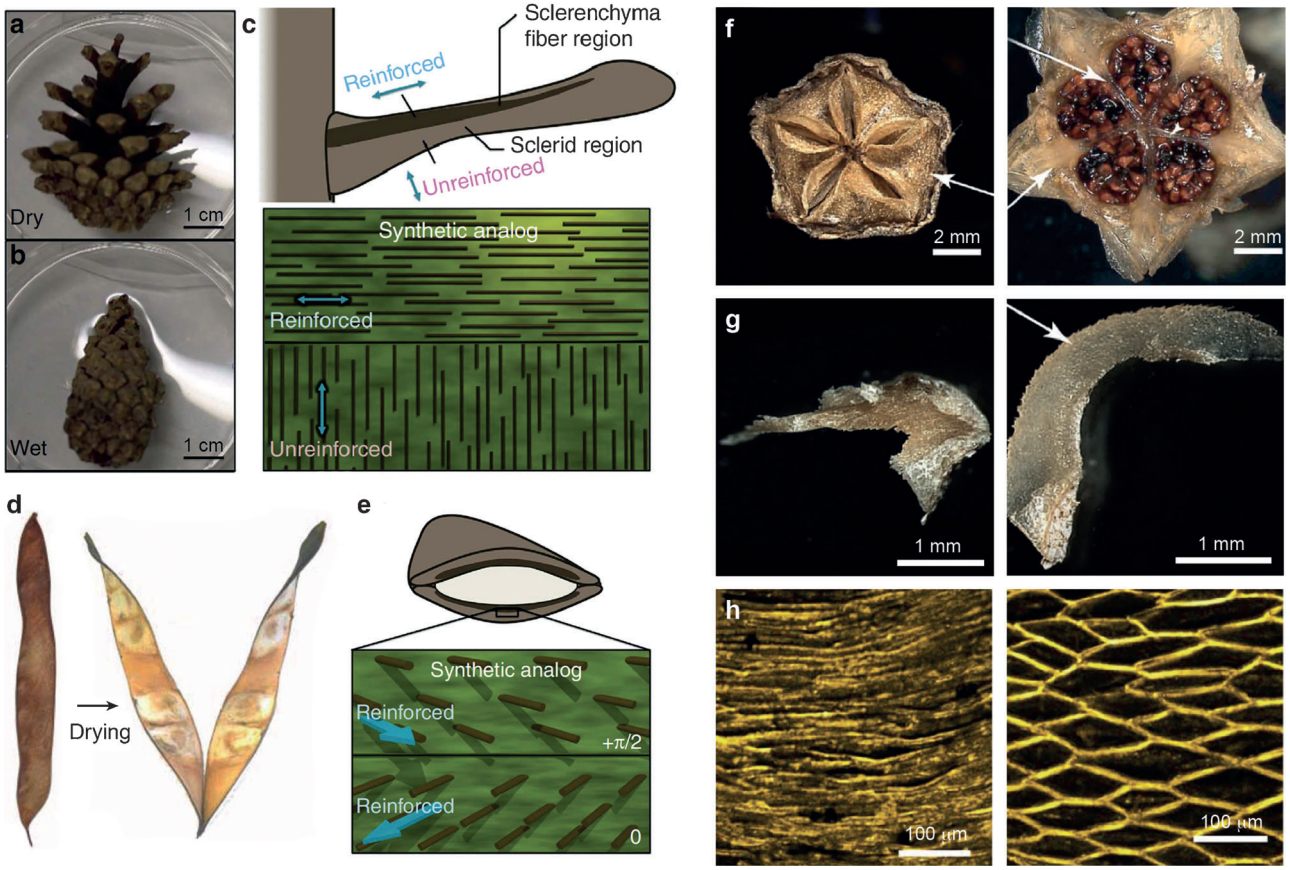

Figure 4. Plant systems displaying autonomous self-shaping behavior.[18,38] a,b) Conifer pinecone that bends its valves outwards upon drying. c) Simplified description of the reinforcement architecture of a pinecone scale. d) Chiral seedpod that twists its valves upon drying. e) Simplified description of the reinforcement architecture of the chiral seedpod valve. (a)–(e) were adapted with permission from Erb et al.[18] f) Opening of the five valves of an ice-plant seed capsule upon hydration. The arrow in the left image indicates the keel that lies along the central axis of each one of the valves. The top and bottom arrows in the right image show, respectively, the keel and the septum that separates different seed compartments. g) Shape change of an individual keel upon hydration. h) Hydration-induced anisotropic expansion of the cellular structure responsible for the shape change of the keel. (f)–(h) were adapted with permission from Harrington et al.[38]

active swelling tissue, known as keel, is found along the central axis of each one of the five opening valves that protect the seed compartments. Such a configuration of active swellable keels present in specific locations of otherwise passive valves makes the shape change of the ice-plant capsules look like origami folding. In this biological origami structure, the keel plays the role of an active hinge that expands by a factor of 4 in the direction of the valve's long axis to unfold the initially closed valve. This highly directional expansion takes only tens of minutes and arises from the anisotropic shape of the hexagonal cells that constitute the keel tissue. Calculations based on the geometry and materials properties of these cells suggest that the keel tissue is 5500 times softer in the direction parallel to the valve's long axis than in the transverse direction. Unidirectional swelling of the keel tissue is caused by the nanoscale solvation of cellulosic material deposited in the inner surfaces of the hexagonal cells (Figure 4 h) and the microscale anisotropy of such cellular structures. The reversible nature of this swelling process makes the ice-plant seed capsule a unique example of a dynamic material system with autonomous self-folding functionality.

The implementation of autonomous self-shaping features in synthetic material systems has been pursued by several research groups over the last decade.[44–53] Similar to the synthetic hair sensorial constructs discussed above, the manufacture of the first origami-like folding structures largely benefited from the use of established soft lithographic processes for the fabrication of multimaterial layered films. Examples of thin-film material architectures that result in autonomous self-shaping behavior are illustrated in Figure 5 a. In the simplest multimaterial configuration, bilayers consisting of two polymer layers exhibiting different swelling behavior can undergo bending upon solvation or temperature changes. Photolithographic deposition of such bilayers at specific locations of the film enables the creation of hinges, which will locally bend in response to an external trigger to allow for controlled origami-like folding similar to that observed in ice-plant seed capsules (Figure 4 f–h). In addition to such equilibrium configurations, shape changes are also possible if the swelling of homogeneous films occurs heterogeneously because of geometrical constraints on the diffusion of solvent. This is the case, for example, when the solvation and swelling of the back surface of the film is kinetically

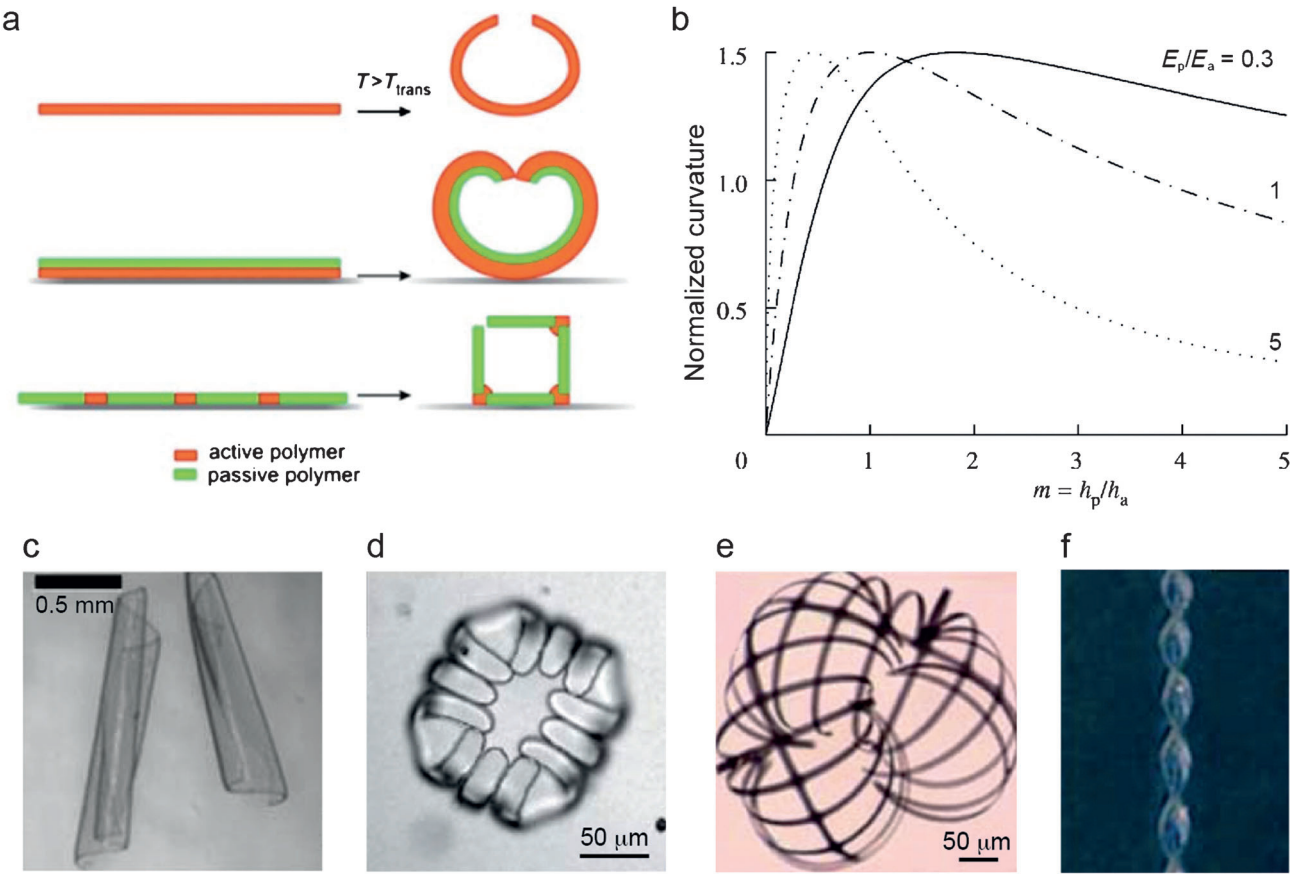

Figure 5. Synthetic self-shaping films made by soft photolithography.[44,47–51] a) Shape-changing mechanisms arising from the heterogeneous expansion of a polymer film (top) or differential expansion of bilayer (middle) or patterned hingelike (bottom) multimaterial systems. Adapted with permission from Ionov.[44] b) Calculated curvature of bilayer films as a function of the relative thickness and relative elastic modulus of the passive and active layers. Adapted with permission from Reyssat et al.[47] (c)–(f) Examples of intricate shapes that can be generated from lithographically made material systems in the form of thin films. Reprinted with permission from c) Simpson et al.,[48] d) Guan et al.,[49] e) Kelby et al.,[50] and f) Jeong et al.[51]

hindered by the substrate to which the film is attached. The bent shapes in equilibrium can be reasonably predicted by using well-established theory for bilayer thermostats (Figure 5b), whereas shape changes that are kinetically controlled require a detailed analysis of the diffusion profiles or temperature distribution around the film.[54]

Besides film bending and rolling (Figure 5c), other unique shape changes are possible by using such a soft lithographic approach.[48–51] For example, when part of the film remains attached to the substrate, structures with multiple reversibly active valves can be constructed to enable controlled capture and release of objects (Figure 5d). Layered films can also be designed to undergo hierarchical bending and thus generate complex architectures, such as that shown in Figure 5e. Even twisted configurations can be fabricated by changing the relative thickness of the different polymers along the length of a bilayer film (Figure 5f). Some of these autonomous shape-changing systems have been explored in biomedical applications for the controlled capture and release of cells, particles, and drugs.[44]

Although soft lithography is a powerful and established approach to fabricate self-folding thin films, most materials obtained through this route lack the three-dimensionality and the biodegradability made possible by the programmable fiber architectures of shape-changing plant systems. To address this limitation, an alternative approach has been developed to generate dynamic self-shaping systems from programmable reinforcement architectures.[18] Similar to the architecture of plant tissues, this method relies on the controlled orientation of reinforcing stiff particles in a common swellable matrix as a means to program and drive shape changes. In this case, anisotropic particles in the form of platelets or short fibers are first suspended in a liquid phase and then oriented in deliberate directions with the help of an external magnetic field. To enable a magnetic response of a typically nonmagnetic reinforcement, the surface of the anisotropic particles is decorated with low concentrations of superparamagnetic iron oxide nanoparticles (SPIONs).[19,55,56] The liquid phase can be a monomer or polymer solution that gels or reacts upon temperature changes to fix the orientation of the magnetically aligned particles. By using platelets and fibers in the micrometer range, orientation control is possible using magnetic fields as low as 10 milliTesla and minimal SPION concentrations in the range of 0.01–0.1 wt%.

Self-shaping reinforced microstructures are created by preparing bilayers that consist of a swellable polymer matrix

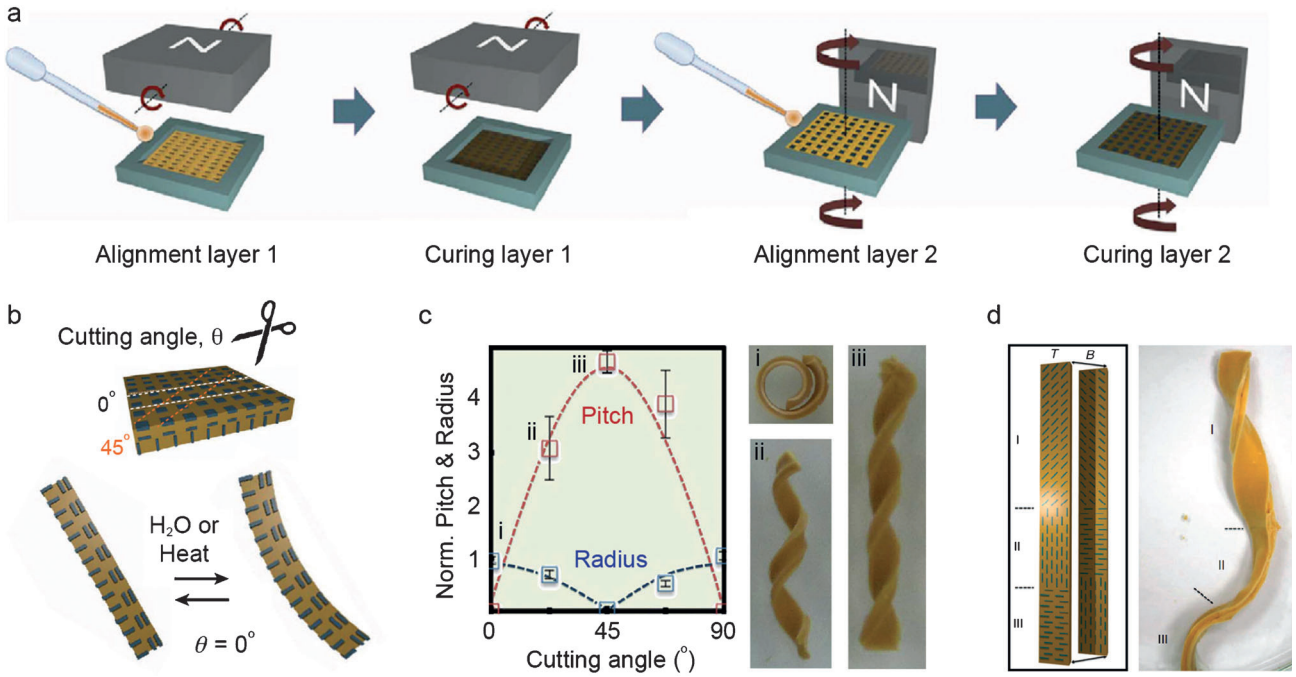

Figure 6. Synthetic self-shaping composites made through the alignment of platelets into bio-inspired reinforcement architectures.[18] a) The sequential magnetic alignment of platelets and gelling of the liquid phase required to obtain reinforced bilayers with anisotropic expansion. b) Reversible shape-changing effects achieved by the hydration or heating of stripes cut from bulk bilayers. c) Effect of the cutting angle on the pitch and radius of the final platelet–hydrogel composite. d) Example of multiple shape changes programmed into the architecture of a single composite part. Adapted with permission from Erb et al.[18]

containing anisotropic particles aligned in different orientations in each of the layers (Figure 6). This is achieved through the sequential casting, magnetic alignment, and matrix consolidation of each individual layer, as depicted schematically in Figure 6a. By using bilayer strips with orthogonally aligned anisotropic particles, a wide range of self-shaping geometries can be achieved upon swelling or shrinkage of the polymer matrix in response to humidity or temperature shifts.

The final shape can be controlled by changing, for example, the direction of the reinforcement relatively to the long axis of the strip, as determined by the angle at which the orthogonally reinforced bilayer strip is cut (Figure 6b). A cutting angle of 0° results in a microstructure similar to that found in pinecones, eventually leading to bending of the strip when the matrix is swollen in water (Figure 6c.i). Conversely, a cutting angle of 45° reproduces the fiber architecture of the chiral seedpod, which causes the bilayer strip to autonomously twist upon hydration and swelling of the matrix (Figure 6c.iii). Helicoidal shapes resulting from a combination of bending and twisting can be achieved at intermediate cutting angles (Figure 6c.ii). The final pitch and radius of curvature of such shape-changing composites can be successfully predicted using energy minimization analytical models (Figure 6c).[18,41] The autonomous shape-changing effect is completely reversible and can be doubly triggered by both hydration and temperature if thermosensitive poly(*N*-isopropylacrylamide) is used as the polymer matrix. Moreover, the reinforcement architecture can be made site-specific such that distinct programmed shape changes can be generated within the same composite material (Figure 6d). As this bio-inspired self-shaping mechanism relies on the architecture of the material at the microscale, it can potentially be combined with the atomic/molecular phase transitions of shape-memory metallic alloys and polymers to provide multiple shape-changing effects in a single dynamic material system. A major advantage of programming self-shaping through the reinforcement architecture is that it is applicable to a very broad variety of chemical processes, thus opening the possibility to create autonomous shape-changing materials from entirely biodegradable and bioresorbable building blocks.

As with the biological counterparts, the macroscopic shape-change effects in the above artificial systems require the solvation effect at the nanoscale combined with the layered, patterned, or anisotropically reinforced structure at the microscale.

In another research direction, reinforced swellable hydrogels have been exploited extensively to create nano- and microstructured surfaces that exhibit unique dynamic functionalities and adaptive properties.[57] In such surface-based DynMatS, the material system consists of arrays of lithographically made high-aspect-ratio (HAR) elements embedded in a continuous environmentally sensitive hydrogel (Figure 7). The mechanism of action and functionalities of such dynamic materials system are different from what was described above for the bulk reinforcement architectures. Instead of imposing an anisotropic swelling of the matrix in a bulk bilayer structure, most surface-based DynMatS rely on the actuation of surface-anchored posts or fins by the triggered contraction of the surrounding confined hydrogel. By using this fundamental principle, the hydrogel-embedded

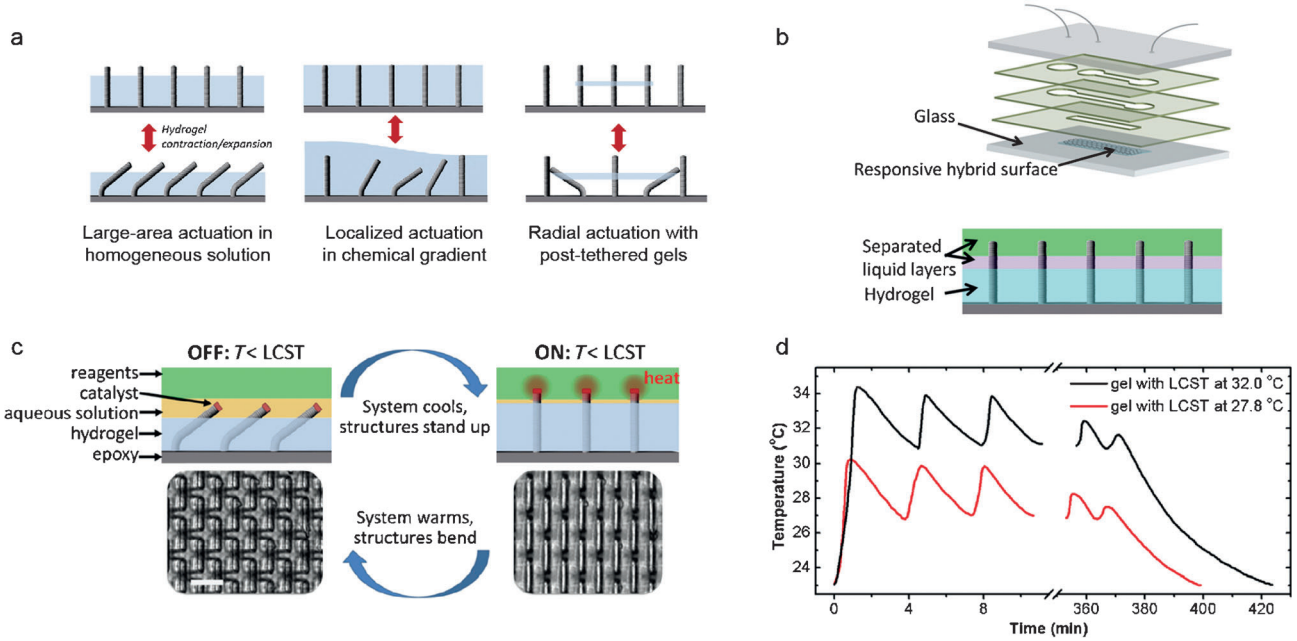

Figure 7. Synthetic material system exhibiting homeostatic behavior through the self-regulated actuation of fin elements.[57,59] a) Modes of actuation of synthetic systems comprising high-aspect-ratio (HAR) elements within a hydrogel matrix. b) Implementation of a microfluidic approach to flow separate liquid layers on top of the responsive hybrid surface. c) The self-regulating mechanism that leads to repeated deflection and recovery of HAR elements driven by the chemically triggered cyclic contraction of the hydrogel matrix. d) Temperature variation between well-defined upper and lower bounds as a result of the homeostatic response of the hybrid system. Reprinted with permission from Zarzar et al.[57]

HAR structures can exhibit three basic modes of actuation: large area coordinated bending, localized bending in specific areas, and localized radial bending (Figure 7a). The coordinated bending of asymmetric fin structures has been demonstrated upon homogeneous chemical stimulus by using hydrogels that are chemically tethered to both the HAR elements and the basal surface.[58] Depending on the hydrogel chemistry, actuation can be triggered by hydration (e.g. polyacrylamide), pH shifts (e.g. poly(acrylic acid-*co*-acrylamide)) or temperature changes (e.g. poly(*N*-isopropylacrylamide). To ensure that the forces generated during hydrogel contraction eventually results in bending, the HAR elements have to be made sufficiently compliant by using either metal elements (e.g. Si) with very high aspect ratios or soft flexible polymers (e.g. epoxies, polyurethanes, polydimethylsiloxane). The mechanical actuation of HAR elements through the chemically triggered contraction of hydrogels has been extensively exploited for the creation of unique functional surfaces with switchable wetting, optical, and chemomechanical responses.[57]

DynMatS based on HAR elements and responsive hydrogels were recently combined with microfluidic tools to generate a self-regulating device displaying a chemo-mechanochemical feedback loop that resembles the homeostatis of biological systems (Figure 7b–d).[59] The device comprises an array of structural fins within a thermoresponsive hydrogel film, which is positioned at the bottom of a microfluidic channel (Figure 7b). The tip of each fin is functionalized with a platinum catalyst that can react with chemicals present in the surrounding liquid media (Figure 7c). The liquid media consists of two coflowing fluids that are pumped through the microfluidic channel under laminar flow conditions. By localizing the reactive chemical into the fluid that is furthest away from the substrate, the reaction with the catalyst is only possible when the fin is stretched out into the far-reaching liquid phase. Under such a stretched configuration, the exothermic reaction takes place and increases the local temperature above the lower critical solution temperature (LCST) of the hydrogel. As a result, the hydrogel contracts and bends the fin structures such that the tips are moved away from the reactive fluid. Thermal equilibration eventually decreases the temperature of the system, thereby allowing the hydrogel to expand and the structural fins to stand up again. This closes up the loop and reinitiates the chemo-mechano-chemical cascade of events, ultimately enabling self-regulation of the system temperature between well-defined upper and lower boundaries (Figure 7d). Despite the need for the active pumping of the fluids, this elegant concept illustrates how a synthetic material system can be designed to dynamically influence the surrounding environment through a self-regulated process. Such a system also provides another proof-of-concept on how an adaptive response can be achieved by combining the intrinsic solvation effect of gels at the nanoscale with a tailored reinforcement architecture at the microscale.

4. Synthetic Dynamic Capsules

Although synthetic materials with self-shaping features and self-regulating adaptive responses can be achieved in the absence of cellular control, the more sophisticated dynamic

functionalities found in biological systems strongly rely on the coordinated action of living cells. Despite the unparalleled complexity of biological systems, major efforts have been made to generate engineered constructs that partly replicate just a few key features of the fascinating dynamic and interactive response of living cells.[60–83] In synthetic biology approaches, cells are often engineered so that the biological molecular machinery is at a minimum while still maintaining selected, key functionalities.[60,61] Research has also been dedicated to the assembly of synthetic microcompartments that are not necessarily connected with biology, but could possibly reproduce some of the essential functionalities of living cells, such as compartmentalization, replication, metabolism, energization, and evolutionary capacity.[61] In this context, nano- and microcapsules with shells consisting of polymers[62–72,83] (polymersomes), lipids[73–80] (liposomes), or colloidal particles[81,82] (colloidosomes) have been extensively investigated in recent years as possible means to generate compartmentalized chemical environments. Here, we discuss two selected examples of recently reported colloidosomes that capture the fundamental concept of compartmentalization that is essential for living cells to perform dynamic functions and thus interact with the surrounding environment.

Compartmentalization allows living cells to accumulate chemicals and build concentration gradients that would not exist in purely diffusive open systems. To perform different functions, these chemical gradients are manipulated by controlling the transport of chemicals across the compartment wall. Cells actively control chemical gradients by decorating their phospholipid bilayer membrane with protein assemblies that function as molecular gates for the selective transport of ions.

A synthetic cell analogue that replicates such a gating concept in a completely different material system has recently been developed by using inorganic hollow capsules with semipermeable colloidal shells, also known as colloidosomes (Figure 8).[81] The semipermeable shell is formed by close-packed silica nanoparticles that were initially assembled on

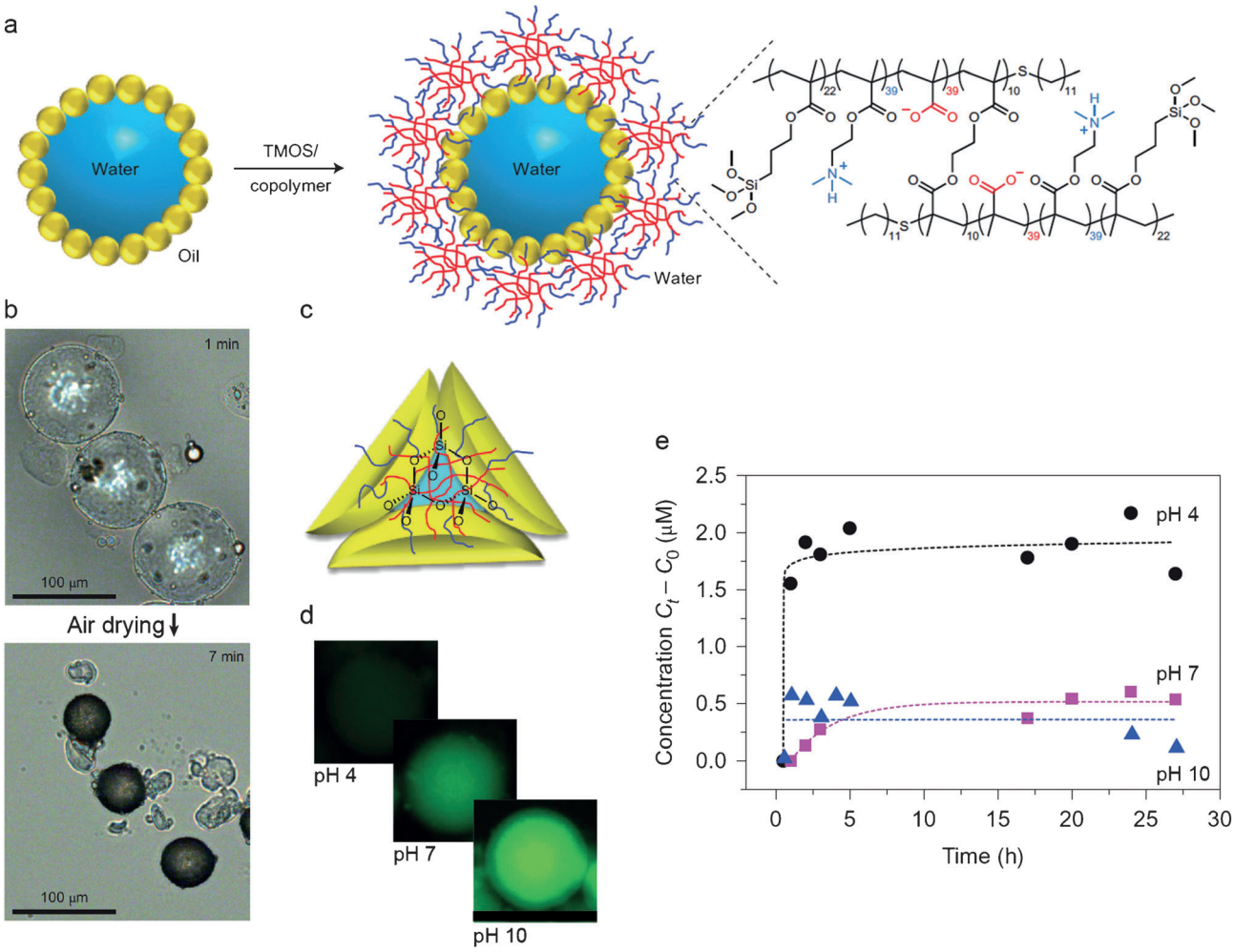

Figure 8. Inorganic colloidosomes that enable controlled molecular transport across the shell by electrostatic gating.[81] a) The assembly process of colloidosomes and their functionalization with a cross-linked copolymer coronal layer. b) Optical micrograph of the obtained colloidosomes, illustrating their mechanical stability upon drying. c) Schematic representation depicting the copolymer layer that electrostatically controls the transport of small molecules across the interstices between shell particles. d,e) Fluorescence microscopy images (d) and concentration of released dye (e) for colloidosomes initially loaded with the negatively charged dye calcein and exposed to aqueous media at different pH values. Reprinted with permission from Li et al.[81]

the surface of a water droplet in a Pickering emulsion. After cross-linking them in place by using sol–gel chemistry, the nanoparticles were surface-modified through covalent binding of a pH-sensitive branched copolymer containing carboxylate, amine, and silanol moieties, as depicted in Figure 8a. The copolymer is designed to form a coronal layer around the colloidosome that can electrostatically control the permeation of small molecules through the interstices between the silica nanoparticles of the shell. The obtained microcapsules could be easily transferred to an aqueous continuous medium and were found to shrink reversibly upon drying in air, thus indicating the high mechanical stability achieved through the inorganic cross-linking and surface-modification procedures (Figure 8b).

The gating properties of the coronal copolymer layer were probed by measuring the transport of initially encapsulated small cationic and anionic fluorescent dyes across the colloidosome membrane (Figure 8c,d). Solute molecules are expected to be blocked by the coronal copolymer layer under pH conditions that result in molecules with equal charge signs. Conversely, transport should take place when the solute molecules and grafted copolymer have opposite charges. Zeta potential measurements show that the capsules have an isoelectric point at a pH value of around 5. Thus, the coronal layer is positively and negatively charged below and above this pH value, respectively. Transport across the capsule membrane was quantified by measuring the release of fluorescent dye from the colloidosome interior to the continuous aqueous phase (Figure 8e). In accordance with the proposed electrostatic gating mechanism, continuous release of the negatively charged dye calcein is observed at a pH value of 4, when the coronal layer is positively charged. In contrast, at pH values of 7 and 10, the negatively charged membrane copolymer blocks the transport of the negatively charged solute across the membrane. This pH-controlled electrostatic gating mechanism leads to microcapsules that can release chemical signals multiple times in response to a well-defined chemical stimulus. Such a colloidosome illustrates the potential of the compartmentalization approach to generate reversibly responsive microcapsules for future adaptive dynamic material systems.

In addition to electrostatic gating, compartmentalization and controlled transport of chemicals across semipermeable colloidosomes has also been achieved through the physical entrapment of cargo-laden colloidal particles within the microcapsule.[82] This concept relies on the design of colloidosome shells with interstitial sizes programmed to allow the permeation of small cargo molecules but restrict the transport of larger colloidal particles, as schematically illustrated in Figure 9a. In such a system, cargo molecules initially adsorbed on the surface of entrapped particles can be controllably released only under chemical conditions that promote their desorption from the large anchoring particles. The on-demand release of cargo molecules can take place multiple times until their concentration inside the capsule is too low to form a chemical gradient with the outer environment. Exposure of the colloidosomes to environments rich in the cargo molecules of interest enables reloading of the system through further adsorption onto the trapped colloids.

This compartmentalization concept was recently demonstrated using colloidosomes prepared from double emulsion templates obtained by a microfluidic route.[82] In contrast to Pickering emulsions, the shells of colloidosomes generated from double emulsions consist of multilayers of close-packed particles rather than a single colloidal layer. This makes the capsules more mechanically robust and the permeability of the shell less sensitive to the inevitable packing defects and inhomogeneities in the particle layer. Multilayered shells are formed by dispersing colloidal nanoparticles in the middle oil phase of water-oil-water double emulsions (Figure 9b). Controlled evaporation of the oil phase enables assembly of the colloidal particles into close-packed arrays, thereby giving rise to a colloidosome shell with a well-defined structure and permeability. The thickness of the shell can be tuned by changing the concentration of the colloidal particles initially dispersed in the oil phase of the double emulsion template.[94,95] In addition to the small particles that will later constitute the capsule wall, the double emulsion is also loaded with larger particles in the innermost aqueous phase to generate the entrapped colloids after consolidation of the shell. In proof-of-concept experiments, Al_2O_3 nanoparticles were used as entrapped colloids to adsorb negatively charged cargo molecules at pH values lower than its isoelectric point of 9 and release them at higher pH values. To quantify the controlled release enabled by such microcapsule constructs, the fluorescent dye calcein was used as a model molecular cargo. When exposed to an acidic environment (pH 5), the negatively charged cargo remains electrostatically adsorbed on the surface of the entrapped Al_2O_3 particles, thereby keeping the capsules in a "dormant state" (Figure 9a,c). An increase of the pH value to 10 inverts the surface charge of the entrapped particles and thus provides the chemical signal required to release the molecular cargo from the active colloidosomes. On-demand switching between the dormant and active states has been demonstrated for at least five cycles, after which reloading of the colloidosome with new cargo is required. Although it deviates markedly from the mechanisms used by living cells to control molecular traffic in biological environments, this compartmentalization approach can offer a simple but effective means to enable chemical signaling in future adaptive DynMatS. Moreover, such chemoresponsive systems provide another example in which nanoscale effects (electrostatic gating and surface adsorption) are combined with a microscale architecture (compartment and semipermeable walls) to generate a unique dynamic material system.

5. Bone as the Ultimate Example of a Structural Dynamic Material System

The remarkable ability of individual living cells to sense, interact with, and control the surrounding environment is harnessed in higher organisms to construct tissues and organs with impressive dynamic properties. In this context, bone is a fascinating example of a cell-controlled material system with dynamic functionalities that find no counterparts in any synthetic material.[84–88] As opposed to most man-made

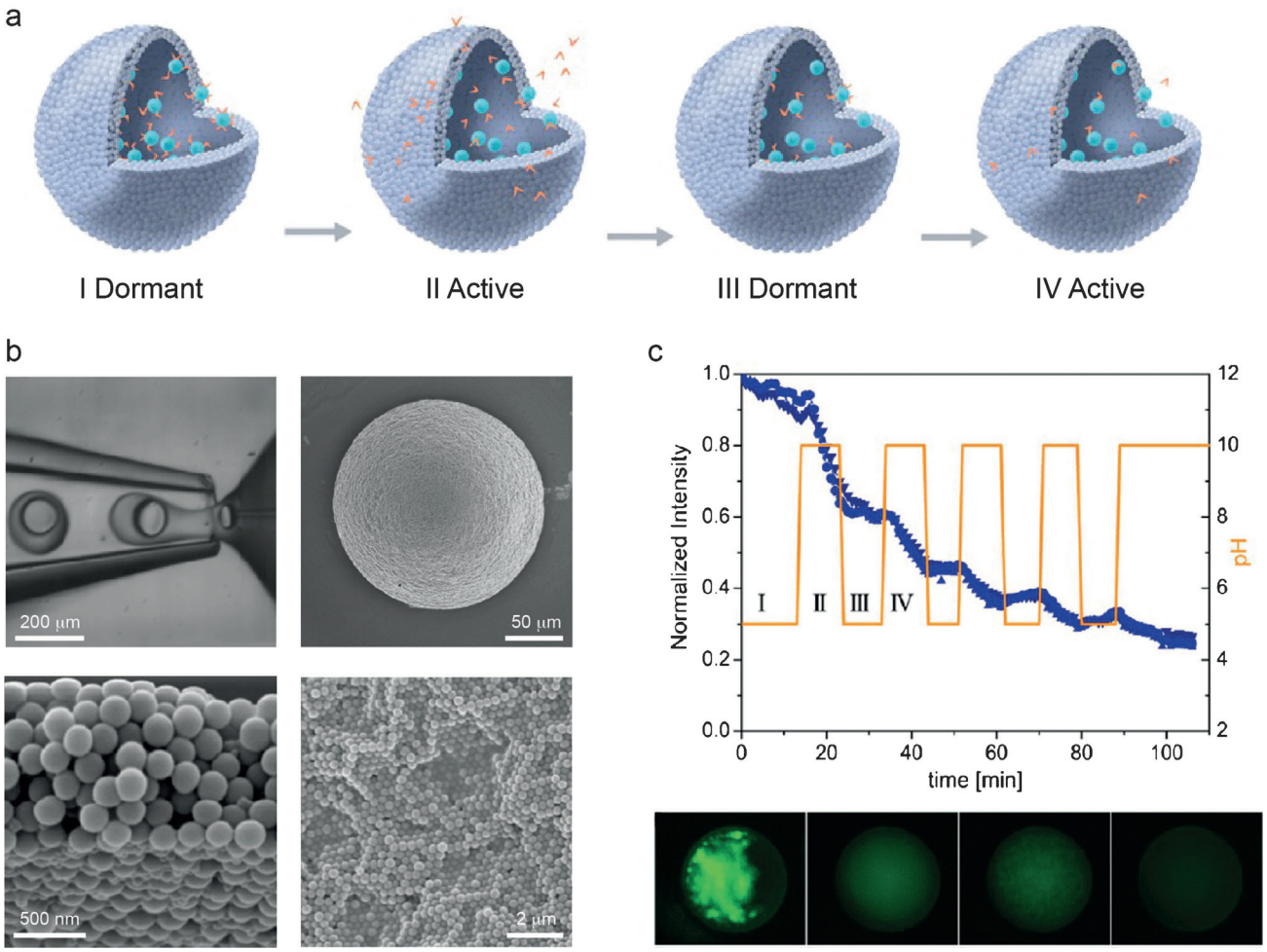

Figure 9. Colloidosomes exhibiting on-demand release properties through the electrostatically mediated physical entrapment of cargo.[82] a) Schematic representation of a colloidosome at multiple dormant and active states, indicating the release mechanism by desorption of cargo from entrapped particles. Large blue spheres represent the entrapped particles, whereas the small orange symbols indicate the cargo molecules. b) Microfluidic double emulsification process utilized for the preparation of multiwalled colloidosomes (top row). Cross-section of the multilayered shell and overview of the outer surface of a colloidosome (bottom row). c) Multiple release of a fluorescent dye from colloidosomes exposed to cyclic variations of the pH value of water. The graph indicates the intensity of the fluorescent dye inside the microcapsule and the bottom images shows fluorescence micrographs of the colloidosome during pH cycles (stages I to IV). (b,c) were adapted with permission from Sander et al.[82,95]

structural parts, bone is a "living material system" that is modeled during growth to become stronger only in those locations subjected to the highest mechanical loads.[89] This phenomenon, known as Wolff's law, enables our skeleton to become strong enough to effectively carry our body mass, but at the same time sufficiently light to minimize the energy cost associated with locomotion. In addition to such an economical growth concept, internal microcracks arising from the cyclic loading imposed by walking and exercising are constantly monitored and eventually fixed through a remarkable process called bone remodeling (Figure 10). This process is controlled by an agglomerate of cells or "minitissue" known as the bone multicellular unit (BMU in Figure 10c).[90–92] Besides connective cells, precursor cells, and nurturing blood capillaries, BMUs contain two cell types that are crucial for bone remodeling: the osteoclasts and the osteoblasts. Together with osteocytes embedded in the bone extracellular matrix, osteoclasts and osteoblasts sense and transmit chemical signals in a highly orchestrated manner in space and time to enable the detection of overstressed damaged locations, removal of damaged bone, and deposition of new healthy bone.

The remodeling process is triggered by the damage or fluid-induced shearing of osteocytes embedded in the highly mineralized bone matrix, as schematically indicated in Figure 10d. In response to such a mechanical stimulus, osteocytes initiate a cascade of chemical signals that ultimately lead to the formation of a BMU close to the highly stressed location of the bone. A BMU is organized such that osteoclasts populate its front end and osteoblasts line both sides of its back. Triggered through chemicals released from osteocytes, osteoclasts at the front of the BMU promote bone dissolution by locally acidifying the extracellular matrix with the help of cellular proton pumps (Figure 10e). This causes the BMU to slowly excavate the damaged bone and move throughout the material like a tunnel-boring machine. The osteoblasts that

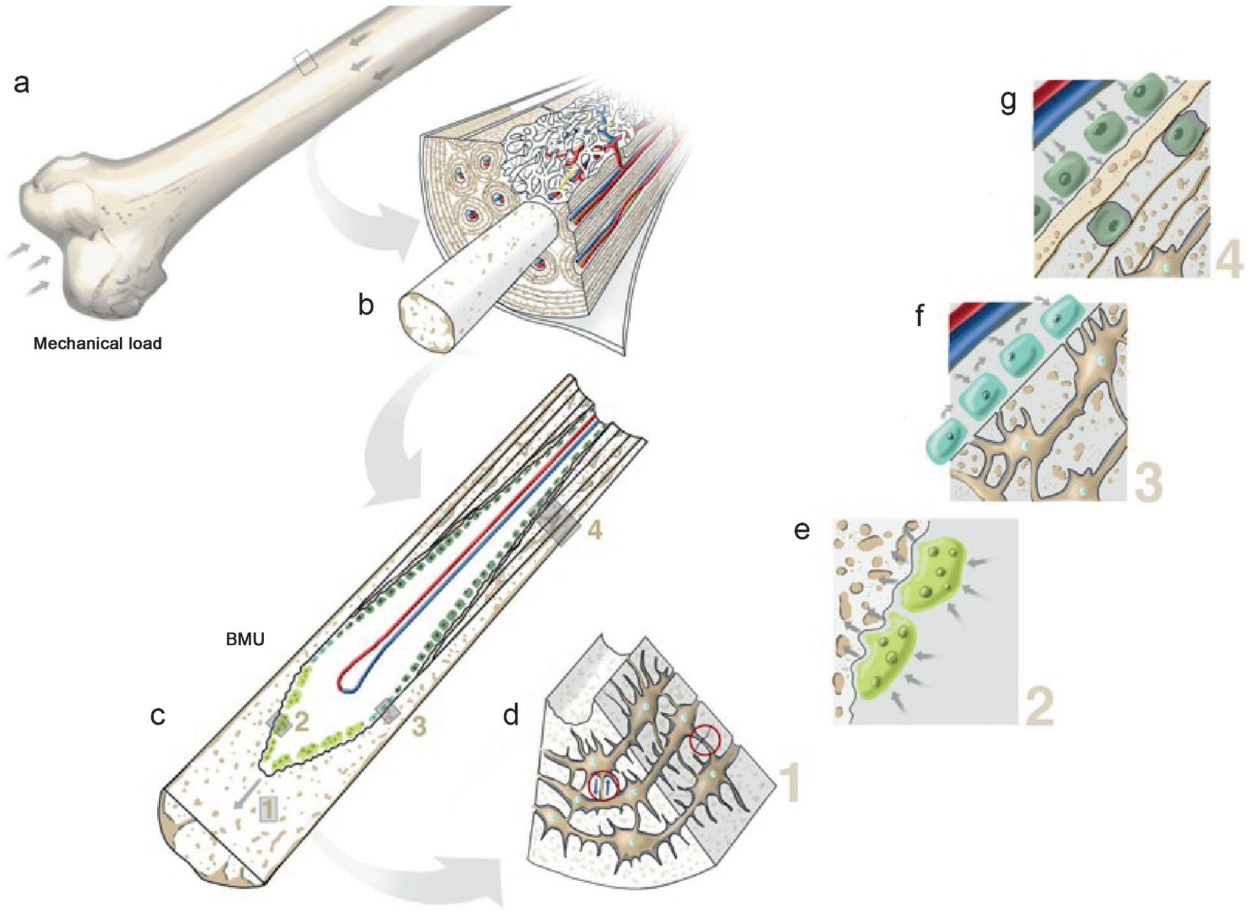

Figure 10. Schematic representation illustrating the remodeling process in bone. a) Femural bone subjected to mechanical load. b) Detailed view of cortical bone, highlighting a region that is microdamaged or that is locally highly stressed. c) Basic multicellular unit (BMU) formed to remodel the damaged or overstressed region. d) High local stress and microdamage is sensed through local shear stresses or rupture of osteocytes embedded in the bone extracellular matrix (red circles). e) In response to chemical signals initiated by osteocytes, osteoclasts locally acidify and dissolve bone at the front end of the BMU. The arrows indicate input and output chemical signals. f) Reversal cells positioned further along the BMU surface take part in the chemical signaling process to prepare the bone surface and call osteoblasts for the deposition of new bone. g) Osteoblasts at the rear of the BMU deposit new bone layers and occasionally become entrapped within the layers to later generate a new osteocyte.

line the back of the BMU secrete chemicals that promote deposition of multiple layers of a collagen matrix (osteoid) that are later mineralized to generate new bone (Figure 10g). Some of the osteoblasts are entrapped within the deposited extracellular matrix to later originate new osteocytes. The coordinated actions of bone-resorbing osteoclasts at the front and bone-depositing osteoblasts at the back are presumably possible with the help of the chemical signaling of so-called reversal cells that occupy the middle region of the BMU (Figure 10f).[93] Blood capillaries that permeate the BMU bring nutrients and precursor cells that can differentiate into osteoblasts or osteoclasts during the remodeling process.

The complex cascade of multiscale events leading to bone remodeling depends strongly on the ability of living cells to sense mechanical or chemical stresses and to pass on targeted instructions through additional chemical signals.[85,93] Despite the unparalleled level of complexity of living cells, current attempts to create synthetic microcapsules that can reversibly release chemicals in response to mechanical or chemical stimuli from the environment might one day in the future enable the development of more complex tissue-like DynMatS that replicate in a very primitive fashion some of the basic adaptive and remodeling functionalities of living tissues such as bone.

6. Conclusions and Outlook

The fascinating adaptive response and dynamic functionalities of biological structures has inspired the creation of a new generation of dynamic material systems (DynMatS). Several examples of DynMatS have been developed following this bio-inspired approach, including for example highly sensitive arrays of hairlike flow sensors, autonomous shape-changing films and bulk structures, artificial homeostatic systems, and chemoresponsive reversible capsules.

Despite their very distinct nature and end functions, a common feature of all the biologically inspired examples highlighted here is the fact that the dynamics of the system emerges not only from fundamental mechanisms at the

nanoscale but also from interactions between building blocks at the microstructural level. This is the case, for example, of the hairlike flow sensors, which rely on piezoresistive or capacitive effects at the nanoscale combined with the integrated hair element and underlying cantilever/membrane at the microscale. Likewise, shape-changing and adaptive hydrogel-based systems require nanoscale solvation effects in combination with mechanical coupling between stiff elements and the surrounding polymer matrix at the microlevel. Finally, chemoresponsive capsules combine electrostatics-driven molecular gating and adsorption at the nanoscale with the formation of semipermeable walls and microcompartments at the microscale.

The intimate integration of building blocks at the microscale clearly distinguishes these bio-inspired systems from manually assembled adaptive and smart macrostructures.[96] Such integration requires the utilization of manufacturing technologies that are applicable to a broad range of organic and inorganic building blocks and that enable their organization into tailored nano- and microstructures. The crucial role of manufacturing technologies in the development of such material systems is evidenced by the fact that many of the DynMatS discussed here, such as the hairlike sensors, the self-folding origami, and the homeostatic self-regulatory device, are fabricated by utilizing mature and well-established lithographic techniques. This clearly indicates that significant future advancements in the creation of dynamic material systems require further developments in processing and manufacturing. Additive manufacturing methods will probably provide additional top-down means to control the geometry and chemistry of building blocks at decreasing length scales, as evidenced, for example, by recent work on the creation of magnetically actuated nanorobots that mimic the swimming behavior of flagellated bacteria.[97] More intricate DynMatS comprising an even higher number of hierarchical levels will likely arise from the combination of top-down fabrication techniques with bottom-up assembly approaches.

The potential of bottom-up colloidal approaches in generating DynMatS with special architectures is illustrated by the successful creation of self-shaping reinforced composites and chemosensitive microcapsules by using self- and directed-assembly strategies. On-going research on soft matter and colloidal systems will increase the repertoire of building blocks and directed assembly routes available for the preparation of advanced DynMatS. Enticing opportunities can be envisioned by exploiting, for example, self-propelling colloidal particles[98,99] and self-replicating colloids as functional constituents of future DynMatS.[100,101]

Finally, the assembly of compartmentalized material systems may also greatly benefit from current efforts to create model protocells for protobiology studies. Likewise, synthetic biology approaches to build cell-like vesicles with functional membrane proteins might open exciting possibilities for the creation of adaptive material systems. However, it is important to note that synthetic DynMatS should not be restricted to the chemistry and structure of biological building blocks and systems. Instead, biology ought to be used as a source of inspiration for fundamental design principles that can be implemented into synthetic systems according to the boundary conditions of each specific application. This approach will greatly enhance our chances of success in replicating synthetically some of the fascinating dynamic and adaptive functionalities of biological systems.

The Swiss National Science Foundation (grants 200021_126646 and 200021_135306/1) and ETH Zurich are greatly acknowledged for the financial support to part of the research presented in this Review. Special thanks also to Prof. Alexander Robling (Indiana University, USA) for kindly teaching me some of the basic mechanisms of bone remodeling.

Received: October 16, 2014
Published online: January 12, 2015

[1] M. Schliwa, G. Woehlke, *Nature* **2003**, *422*, 759 – 765.
[2] M. von Delius, D. A. Leigh, *Chem. Soc. Rev.* **2011**, *40*, 3656 – 3676.
[3] H. Lodish, A. Berk, C. A. Kaiser, M. Krieger, M. P. Scott, A. Bretscher, *Molecular Cell Biology*, *6. ed.*, W. H. Freeman, **2007**, pp. 1150.
[4] P. Fratzl, R. Weinkamer, *Prog. Mater. Sci.* **2007**, *52*, 1263 – 1334.
[5] A. J. Moulson, J. M. Herbert, *Electroceramics*, Wiley, New York, **2003**.
[6] J. M. Jani, M. Leary, A. Subic, M. A. Gibson, *Mater. Des.* **2014**, *56*, 1078 – 1113.
[7] A. Lendlein, S. Kelch, *Angew. Chem. Int. Ed.* **2002**, *41*, 2034 – 2057; *Angew. Chem.* **2002**, *114*, 2138 – 2162.
[8] A. F. Arrieta, O. Bilgen, M. I. Friswell, P. Hagedorn, *J. Intell. Mater. Syst. Struct.* **2013**, *24*, 266 – 273.
[9] C. Thill, J. Etches, I. Bond, K. Potter, P. Weaver, *Aeronautical J.* **2008**, *112*, 117 – 139.
[10] L. L. Hench, J. K. West, *Principles of Electronic Ceramics*, Wiley, New York, **1990**.
[11] A. R. Studart, *Adv. Funct. Mater.* **2013**, *23*, 4423 – 4436.
[12] A. R. Studart, *Adv. Mater.* **2012**, *24*, 5024 – 5044.
[13] M. M. Porter, M. Yeh, J. Strawson, T. Goehring, S. Lujan, P. Siripasopsotorn, M. A. Meyers, J. McKittrick, *Mater. Sci. Eng.* **2012**, *556*, 741 – 750.
[14] E. Munch, M. E. Launey, D. H. Alsem, E. Saiz, A. P. Tomsia, R. O. Ritchie, *Science* **2008**, *322*, 1516 – 1520.
[15] S. Deville, E. Saiz, R. K. Nalla, A. P. Tomsia, *Science* **2006**, *311*, 515 – 518.
[16] Z. Y. Tang, N. A. Kotov, S. Magonov, B. Ozturk, *Nat. Mater.* **2003**, *2*, 413-U8.
[17] A. R. Studart, R. M. Erb, *Soft Matter* **2014**, *10*, 1284 – 1294.
[18] R. M. Erb, J. S. Sander, R. Grisch, A. R. Studart, *Nat. Commun.* **2013**, *4*, 1712.
[19] R. M. Erb, R. Libanori, N. Rothfuchs, A. R. Studart, *Science* **2012**, *335*, 199 – 204.
[20] M. Mirkhalaf, A. K. Dastjerdi, F. Barthelat, *Nat. Commun.* **2014**, *5*, 3166.
[21] A. R. Parker, H. E. Townley, *Nat. Nanotechnol.* **2007**, *2*, 347 – 353.
[22] A. Walther, I. Bjurhager, J. M. Malho, J. Ruokolainen, L. Berglund, O. Ikkala, *Angew. Chem. Int. Ed.* **2010**, *49*, 6448 – 6453; *Angew. Chem.* **2010**, *122*, 6593 – 6599.
[23] K. S. Toohey, N. R. Sottos, J. A. Lewis, J. S. Moore, S. R. White, *Nat. Mater.* **2007**, *6*, 581 – 585.
[24] L. Feng, S. H. Li, Y. S. Li, H. J. Li, L. J. Zhang, J. Zhai, Y. L. Song, B. Q. Liu, L. Jiang, D. B. Zhu, *Adv. Mater.* **2002**, *14*, 1857 – 1860.

[25] S. Sengupta, M. E. Ibele, A. Sen, *Angew. Chem. Int. Ed.* **2012**, *51*, 8434 – 8445; *Angew. Chem.* **2012**, *124*, 8560 – 8571.
[26] F. G. Barth, J. A. C. Humphrey, M. V. Srinivasan, *Frontiers in Sensing*: *From Biology to Engineering*, Springer, Amsterdam, **2012**.
[27] "Learning from animal sensors: the clever "design" of spider mechanoreceptors": F. G. Barth in *Proc. SPIE 8339, Bioinspiration, Biomimetics, and Bioreplication*, **2012**, 833904.
[28] P. Fratzl, F. G. Barth, *Nature* **2009**, *462*, 442 – 448.
[29] "Nature as a model for technical sensors": H. Bleckmann, A. Klein, G. Meyer in *Frontiers in Sensing*: *From Biology to Engineering* (Eds.: F. G. Barth, J. A. C. Humphrey, M. V. Srinivasan), Springer, Amsterdam, **2012**, pp. 3 – 18.
[30] M. E. McConney, K. D. Anderson, L. L. Brott, R. R. Naik, V. V. Tsukruk, *Adv. Funct. Mater.* **2009**, *19*, 2527 – 2544.
[31] J. L. Tao, X. Yu, *Smart Mater. Struct.* **2012**, *21*, 113001.
[32] Y. C. Yang, A. Klein, H. Bleckmann, C. Liu, *Appl. Phys. Lett.* **2011**, *99*, 023701.
[33] Y. C. Yang, J. Chen, J. Engel, S. Pandya, N. N. Chen, C. Tucker, S. Coombs, D. L. Jones, C. Liu, *Proc. Natl. Acad. Sci. USA* **2006**, *103*, 18891 – 18895.
[34] C. Liu, *Adv. Mater.* **2007**, *19*, 3783 – 3790.
[35] "Design and fabrication process for artificial lateral line sensors": N. Izadi, G. J. M. Krijnen in *Frontiers in Sensing*: *From Biology to Engineering* (Eds.: F. G. Barth, J. A. C. Humphrey, M. V. Srinivasan), Springer, Amsterdam, **2012**, pp. 405 – 421.
[36] N. Izadi, M. J. de Boer, J. W. Berenschot, G. J. M. Krijnen, *J. Micromech. Microeng.* **2010**, *20*, 085041.
[37] N. Nguyen, D. L. Jones, Y. C. Yang, C. Liu, *Eurasip J. Adv. Signal Processing* **2011**.
[38] M. J. Harrington, K. Razghandi, F. Ditsch, L. Guiducci, M. Rueggeberg, J. W. C. Dunlop, P. Fratzl, C. Neinhuis, I. Burgert, *Nat. Commun.* **2011**, *2*, 337.
[39] R. Elbaum, L. Zaltzman, I. Burgert, P. Fratzl, *Science* **2007**, *316*, 884 – 886.
[40] P. Fratzl, R. Elbaum, I. Burgert, *Faraday Discuss.* **2008**, *139*, 275 – 282.
[41] S. Armon, E. Efrati, R. Kupferman, E. Sharon, *Science* **2011**, *333*, 1726 – 1730.
[42] Y. Forterre, J. M. Skotheim, J. Dumais, L. Mahadevan, *Nature* **2005**, *433*, 421 – 425.
[43] C. Dawson, J. F. V. Vincent, A.-M. Rocca, *Nature* **1997**, *290*, 668.
[44] L. Ionov, *Soft Matter* **2011**, *7*, 6786 – 6791.
[45] D. H. Gracias, J. Tien, T. L. Breen, C. Hsu, G. M. Whitesides, *Science* **2000**, *289*, 1170 – 1172.
[46] D. H. Gracias, V. Kavthekar, J. C. Love, K. E. Paul, G. M. Whitesides, *Adv. Mater.* **2002**, *14*, 235 – 238.
[47] E. Reyssat, L. Mahadevan, *J. R. Soc. Interface* **2009**, *6*, 951 – 957.
[48] B. Simpson, G. Nunnery, R. Tannenbaum, K. Kalaitzidou, *J. Mater. Chem.* **2010**, *20*, 3496 – 3501.
[49] J. J. Guan, H. Y. He, L. J. Lee, D. J. Hansford, *Small* **2007**, *3*, 412 – 418.
[50] T. S. Kelby, M. Wang, W. T. S. Huck, *Adv. Funct. Mater.* **2011**, *21*, 652 – 657.
[51] K. U. Jeong, J. H. Jang, D. Y. Kim, C. Nah, J. H. Lee, M. H. Lee, H. J. Sun, C. L. Wang, S. Z. D. Cheng, E. L. Thomas, *J. Mater. Chem.* **2011**, *21*, 6824 – 6830.
[52] L. Ionov, *Adv. Funct. Mater.* **2013**, *23*, 4555 – 4570.
[53] S. M. Felton, M. T. Tolley, B. Shin, C. D. Onal, E. D. Demaine, D. Rus, R. J. Wood, *Soft Matter* **2013**, *9*, 7688 – 7694.
[54] G. Stoychev, S. Zakharchenko, S. Turcaud, J. W. C. Dunlop, L. Ionov, *ACS Nano* **2012**, *6*, 3925 – 3934.
[55] R. M. Erb, J. Segmehl, M. Schaffner, A. R. Studart, *Soft Matter* **2013**, *9*, 498 – 505.
[56] R. M. Erb, J. Segmehl, M. Charilaou, J. F. Loffler, A. R. Studart, *Soft Matter* **2012**, *8*, 7604 – 7609.
[57] L. D. Zarzar, J. Aizenberg, *Acc. Chem. Res.* **2014**, *47*, 530 – 539.
[58] L. D. Zarzar, P. Kim, J. Aizenberg, *Adv. Mater.* **2011**, *23*, 1442 – 1446.
[59] X. M. He, M. Aizenberg, O. Kuksenok, L. D. Zarzar, A. Shastri, A. C. Balazs, J. Aizenberg, *Nature* **2012**, *487*, 214 – 218.
[60] P. L. Luisi, F. Ferri, P. Stano, *Naturwissenschaften* **2006**, *93*, 1 – 13.
[61] S. Mann, *Acc. Chem. Res.* **2012**, *45*, 2131 – 2141.
[62] B. M. Discher, Y. Y. Won, D. S. Ege, J. C. M. Lee, F. S. Bates, D. E. Discher, D. A. Hammer, *Science* **1999**, *284*, 1143 – 1146.
[63] D. E. Discher, A. Eisenberg, *Science* **2002**, *297*, 967 – 973.
[64] F. H. Meng, G. H. M. Engbers, J. Feijen, *J. Controlled Release* **2005**, *101*, 187 – 198.
[65] S. F. M. van Dongen, H. P. M. de Hoog, R. Peters, M. Nallani, R. J. M. Nolte, J. C. M. van Hest, *Chem. Rev.* **2009**, *109*, 6212 – 6274.
[66] J. Gaitzsch, D. Appelhans, L. G. Wang, G. Battaglia, B. Voit, *Angew. Chem. Int. Ed.* **2012**, *51*, 4448 – 4451; *Angew. Chem.* **2012**, *124*, 4524 – 4527.
[67] M. Marguet, C. Bonduelle, S. Lecommandoux, *Chem. Soc. Rev.* **2013**, *42*, 512 – 529.
[68] D. Gräfe, J. Gaitzsch, D. Appelhans, B. Voit, *Nanoscale* **2014**, *6*, 10752 – 10761.
[69] H. J. Choi, C. D. Montemagno, *Nano Lett.* **2005**, *5*, 2538 – 2542.
[70] P. Broz, S. Driamov, J. Ziegler, N. Ben-Haim, S. Marsch, W. Meier, P. Hunziker, *Nano Lett.* **2006**, *6*, 2349 – 2353.
[71] A. Blanazs, S. P. Armes, A. J. Ryan, *Macromol. Rapid Commun.* **2009**, *30*, 267 – 277.
[72] H. C. Shum, J. W. Kim, D. A. Weitz, *J. Am. Chem. Soc.* **2008**, *130*, 9543 – 9549.
[73] T. Oberholzer, M. Albrizio, P. L. Luisi, *Chem. Biol.* **1995**, *2*, 677 – 682.
[74] T. Oberholzer, R. Wick, P. L. Luisi, C. K. Biebricher, *Biochem. Biophys. Res. Commun.* **1995**, *207*, 250 – 257.
[75] P. Walde, S. Ichikawa, *Biomol. Eng.* **2001**, *18*, 143 – 177.
[76] S. Nomura, K. Tsumoto, T. Hamada, K. Akiyoshi, Y. Nakatani, K. Yoshikawa, *ChemBioChem* **2003**, *4*, 1172 – 1175.
[77] V. Noireaux, A. Libchaber, *Proc. Natl. Acad. Sci. USA* **2004**, *101*, 17669 – 17674.
[78] P. Stano, P. L. Luisi, *Chem. Commun.* **2010**, *46*, 3639 – 3653.
[79] P. Stano, P. Carrara, Y. Kuruma, T. P. de Souza, P. L. Luisi, *J. Mater. Chem.* **2011**, *21*, 18887 – 18902.
[80] J. W. Szostak, D. P. Bartel, P. L. Luisi, *Nature* **2001**, *409*, 387 – 390.
[81] M. Li, R. L. Harbron, J. V. M. Weaver, B. P. Binks, S. Mann, *Nat. Chem.* **2013**, *5*, 529 – 536.
[82] J. S. Sander, A. R. Studart, *Langmuir* **2013**, *29*, 15168 – 15173.
[83] P. Tanner, P. Baumann, R. Enea, O. Onaca, C. Palivan, W. Meier, *Acc. Chem. Res.* **2011**, *44*, 1039 – 1049.
[84] J. D. Currey, *Bones*: *Structure and Mechanics*, Princeton University Press, Princeton, **2002**.
[85] A. G. Robling, A. B. Castillo, C. H. Turner, *Annu. Rev. Biomed. Eng.* **2006**, *8*, 455 – 498.
[86] J. W. C. Dunlop, M. A. Hartmann, Y. J. Brechet, P. Fratzl, R. Weinkamer, *Calcif. Tissue Int.* **2009**, *85*, 45 – 54.
[87] H. M. Frost, *Anat. Rec.* **1987**, *219*, 1 – 9.
[88] R. Weinkamer, P. Fratzl, *Mater. Sci. Eng. C* **2011**, *31*, 1164 – 1173.
[89] J. Wolff, *The Law of Bone Remodelling*, Translated from original German edition from 1892 ed., Springer, Berlin, **1986**.
[90] A. M. Parfitt, *J. Cell. Biochem.* **1994**, *55*, 273 – 286.
[91] C. J. Hernandez, G. S. Beaupre, D. R. Carter, *J. Rehabilitation Res. Dev.* **2000**, *37*, 235 – 244.
[92] N. A. Sims, T. J. Martin, *BoneKEy Rep.* **2014**, *3*, 481.

[93] L. J. Raggatt, N. C. Partridge, *J. Biol. Chem.* **2010**, *285*, 25103 – 25108.
[94] D. Lee, D. A. Weitz, *Adv. Mater.* **2008**, *20*, 3498 – 3503.
[95] J. S. Sander, A. R. Studart, *Langmuir* **2011**, *27*, 3301 – 3307.
[96] H. Janocha, *Adaptronics and Smart Structures*, Springer, Amsterdam, **2007**.
[97] S. Tottori, L. Zhang, F. M. Qiu, K. K. Krawczyk, A. Franco-Obregon, B. J. Nelson, *Adv. Mater.* **2012**, *24*, 811 – 816.
[98] L. Baraban, M. Tasinkevych, M. N. Popescu, S. Sanchez, S. Dietrich, O. G. Schmidt, *Soft Matter* **2012**, *8*, 48 – 52.
[99] Y. Hong, N. M. K. Blackman, N. D. Kopp, A. Sen, D. Velegol, *Phys. Rev. Lett.* **2007**, *99*, 178103.
[100] M. E. Leunissen, R. Dreyfus, R. J. Sha, T. Wang, N. C. Seeman, D. J. Pine, P. M. Chaikin, *Soft Matter* **2009**, *5*, 2422 – 2430.
[101] Z. Zeravcic, M. P. Brenner, *Proc. Natl. Acad. Sci. USA* **2014**, *111*, 1748 – 1753.
[102] S. Coombs, *Autonomous Robots* **2001**, *11*, 255 – 261.